Original Research

Magnetization Transfer (MT) Asymmetry Around the Water Resonance in Human Cervical Spinal Cord

Man-Cheuk Ng, PhD,[1] Jun Hua, MSc,[2,3] Yong Hu, PhD,[4] Keith D. Luk, MD, PhD,[4] and Edmund Y. Lam, PhD[1]*

Purpose: To demonstrate the presence of magnetization transfer (MT) asymmetry in human cervical spinal cord due to the interaction between bulk water and semisolid macromolecules (conventional MT), and the chemical exchange dependent saturation transfer (CEST) effect.

Materials and Methods: MT asymmetry in the cervical spinal cord (C3/C4–C5) was investigated in 14 healthy male subjects with a 3T magnetic resonance (MR) system. Both spin-echo (SE) and gradient-echo (GE) echo-planar imaging (EPI) sequences, with low-power off-resonance radiofrequency irradiation at different frequency offsets, were used.

Results: Our results show that the z-spectrum in gray/white matter (GM/WM) is asymmetrical about the water resonance frequency in both SE-EPI and GE-EPI, with a more significant saturation effect at the lower frequencies (negative frequency offset) far away from water and at the higher frequencies (positive offset) close to water. These are attributed mainly to the conventional MT and CEST effects respectively. Furthermore, the amplitude of MT asymmetry is larger in the SE-EPI sequence than in the GE-EPI sequence in the frequency range of amide protons.

Conclusion: Our results demonstrate the presence of MT asymmetry in human cervical spinal cord, which is consistent with the ones reported in the brain.

Key Words: magnetization transfer; asymmetry; CEST; APT; spinal cord
J. Magn. Reson. Imaging 2009;29:523–528.

THE PROTONS IN SOLID-LIKE MACROMOLECULES and mobile proteins in tissues can be selectively saturated by an off-resonance magnetization transfer (MT) prepulse in magnetic resonance imaging (MRI). It allows indirect detection of solid-like macromolecules through the exchange coupling of magnetization between the spins associated with bulk water and macromolecules by detecting the water signal intensity (1–4). The so-called MT ratio (MTR) and z-spectrum (3) are commonly used to describe the magnitude of MT effect at different frequency offsets. Several quantitative models of MT have been proposed, among which Henkelman's two-pool model is one of the most widely used (5). In many of these models, it has been generally assumed that the resonant frequency of the bulk water is the same as the solid-like macromolecules, which leads to symmetric z-spectra. However, recent research has suggested that this assumption may not be valid. In particular, several studies have demonstrated asymmetrical z-spectra around the water resonance in different tissues (6–13). There are two types of MT asymmetry as reported. The first is associated with the conventional MT effect about the interaction between bulk water and semisolid macromolecules (conventional MT asymmetry) (6–9). It has been pointed out that in the brain, the z-spectra in tissue are slightly asymmetric around the water proton resonance frequency, with the center of the z-spectrum shifted slightly upfield (i.e., toward the lower frequency) from the water resonance (6–8). The second type of MT asymmetry is due to the chemical exchange dependent saturation transfer (CEST) effect associated with exchangeable protons of some side groups, e.g., –OH, –SH, and –NH (10–13). The saturation transfer takes place at a particular frequency corresponding to the MR of the exchangeable protons. The saturated solute protons are replaced repeatedly by the nonsaturated water protons, and when the former accumulate in the water pool, there is saturation amplification (14) leading to an asymmetrical z-spectrum. Understanding the conventional MT asymmetry and CEST is important for clinical purposes, as they can help provide different contrast for certain types of pathology. Recently, it has also been reported that the MT asymmetry in 9L rat brain tumors is different from that in contralateral normal-appearing brain tissue (8,15), which implies the feasibility of using MT asymmetry for tissue characterization as well. In

[1]Department of Electrical and Electronic Engineering, University of Hong Kong, Pokfulam, Hong Kong.
[2]Russell H. Morgan Department of Radiology and Radiological Sciences, Division of MR Research, Johns Hopkins University, Baltimore, Maryland, USA.
[3]F.M. Kirby Center for Functional Brain Imaging, Kennedy Krieger Institute, Baltimore, Maryland, USA.
[4]Department of Orthopedics and Traumatology, University of Hong Kong, Pokfulam, Hong Kong.
Poster presented at the 16th Annual Meeting of ISMRM, Toronto, Canada, 2008, and published as an abstract in the conference proceedings.
*Address reprint requests to: E.Y.L., Department of Electrical and Electronic Engineering, Room 504, Chow Yei Ching Building, University of Hong Kong, Pokfulam, Hong Kong. E-mail: elam@eee.hku.hk
Received May 7, 2008; Accepted August 27, 2008.
DOI 10.1002/jmri.21610
Published online in Wiley InterScience (www.interscience.wiley.com).

the current study, the conventional MT asymmetry and CEST are investigated in human cervical spinal cord using a 3T MR system. It is hoped that these two types of MT asymmetry effects can be verified in the cord as in the brain, which can then serve as the basis for future studies in patients with spinal cord diseases such as tumor and cervical myelopathy. The potential application of the current imaging techniques may facilitate better understanding of certain pathologies in the spinal cord.

MATERIALS AND METHODS

Theory

The z-spectrum plots the ratio of water signal intensities with and without the MT pulse as a function of frequency offset of the radiofrequency (RF) irradiation pulse, i.e., M_{sat}(offset) / M_0 vs. frequency offset of the MT prepulse, where M_{sat}(offset) is the detected water magnetization with MT prepulse at a particular frequency offset, and M_0 is the one without the prepulse. To study the magnitude of the MT effect, the MTR can be calculated using:

$$\mathrm{MTR(offset)} = 1 - M_{sat}(\mathrm{offset})/M_0.$$

The MT asymmetry spectrum can be calculated by subtracting the MTR obtained at the negative offsets with respect to water from those at the corresponding positive offsets. Therefore, MTR_{asym} is defined as:

$$\begin{aligned} &MTR_{asym}(\mathrm{offset}) \\ &\quad = \mathrm{MTR(positive\ offset)} - \mathrm{MTR(negative\ offset)} \\ &\quad = M_{sat}(\mathrm{negative\ offset})/M_0 - M_{sat}(\mathrm{positive\ offset})/M_0 \end{aligned}$$

Subjects

Fourteen healthy male subjects, aged 19 to 29 years (22.4 ± 2.5 years), were recruited in this study. Each participating subject gave fully informed consent prior to the experiment. The protocol was approved by the research ethics committee of the institution where the study was carried out. For screening, sagittal T2-weighted and T1-weighted images were acquired before the study.

Scanning

Subjects were scanned on a 3T MRI scanner (Philips Achieva) with a multielement spine coil as a receive coil and a Q-body coil as the transmit coil. Four axial slices were acquired, with each one placed at either vertebral or disc level from C3/C4 to C5. Single-shot spin-echo echo-planar imaging (SE-EPI) and gradient-echo EPI (GE-EPI) with one MT prepulse (pulse shape: block, saturation power: 2 μT, saturation duration: 500 msec) were used with frequency offsets from −80 ppm to 80 ppm. The frequency step was 5 ppm between 10 ppm and 80 ppm, and 0.5 ppm between 0 ppm and 8ppm. It has been shown that there exists a characteristic RF saturation power (ω_{1c}) that maximizes the conventional MT asymmetry, and it approximately falls in the range of 0.5–3.5 μT at the frequency offsets of 5–60 ppm (7). The saturation power of 2 μT was therefore chosen in this study mainly to keep the specific absorption rate (SAR) at a reasonable level while achieving a considerable amount of conventional MT asymmetry. EPI was used in this study to shorten the imaging time, which would minimize the bulk motion artifacts from the subjects. The short acquisition time for each dynamic also enabled more sampling in the MT frequency offsets spectrum to study the CEST and conventional MT asymmetry effects.

For SE-EPI, the flip angle was set at 90°, and the echo time (TE) was 31 msec. In order to decrease the oblique flow displacement artifact from the cerebrospinal fluid (CSF), the prephasing gradient lobe for phase-encoding was placed after the 180° refocusing pulse (16). For GE-EPI, the flip angle was 70° and TE was 9.7 msec. Other common imaging parameters were as follows: field of view (FOV) = 80 * 36 mm^2, voxel size = 1 * 1.24 * 7 mm^3, repetition time (TR) = 2 heartbeats, number of excitations (NEX) = 1, half scan factor ≈ 0.8, high-order shimming was on, fat saturation was applied, and vectorcardiogram (VCG) triggering was used. The scanning time for SE-EPI and GE-EPI was around eight minutes for each sequence. In order to minimize the susceptibility artifacts in the cervical spinal cord in both SE-EPI and FE-EPI, a small encoding matrix size and FOV were used to shorten the EPI factor. A short TE was used to minimize spin dephasing, and high-order shimming was utilized to achieve higher field homogeneity in the cord. No parallel imaging was used in this study as the spine coil used did not support parallel imaging.

Postprocessing

Two-dimensional rigid-body registration with three degrees of freedom was performed on the data volumes to eliminate the bulk motion effect using the software AIR (17). All the images from the subjects were assessed visually after automatic registration to ensure that the position of the spinal cord in different frequency offsets were well aligned. To minimize the B_0 field inhomogeneity problem, the z-spectrum was interpolated to 1-Hz resolution with curve fitting. The minimum of the fitted z-spectra was assumed to be the water resonant frequency, which was shifted to 0 Hz (7). In addition, the two outermost points in the z-spectra were discarded due to the shifting (7). Two regions of interest (ROIs) were then drawn manually. The first one covered the gray matter (GM) and white matter (WM) of the spinal cord, and the second one covered only the CSF. To minimize the partial volume effect, the ROIs were eroded for 1 voxel. Next, the homogeneity-corrected z-spectral intensities (i.e. the interpolated and shifted raw data) at the corresponding positive and negative offsets around the water proton resonant frequency were compared on a voxel-by-voxel basis, in order to demonstrate the MTR asymmetry effect in the cervical spinal cord. The MTR_{asym} was obtained for both GM/WM and CSF in SE-EPI and GE-EPI sequences.

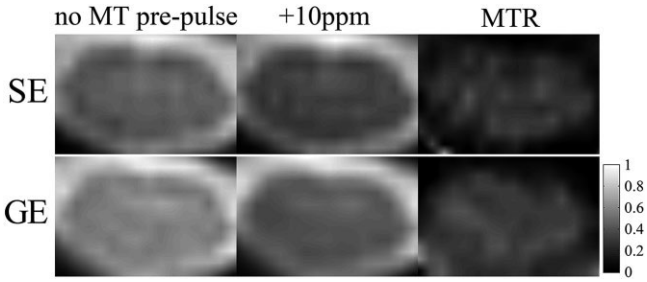

Figure 1. Left: Representative spinal cord images from SE and GE EPI sequences without MT prepulse. **Middle:** SE-EPI and GE-EPI with MT prepulse at frequency offset +10 ppm. **Right:** Corresponding MTR images of the middle column with color bar. The computation of MTR was performed on the raw data right after image registration. (Note: postinterpolation has been done in this figure for better display, to avoid a blocky appearance.)

Statistical Analysis

A one-sample Student's *t*-test was performed on the mean MTR_{asym} values from both SE-EPI and GE-EPI data. This examined whether there was any significant difference from zero at various frequency offsets for the detection of the conventional MT asymmetry and CEST effects in the GM/WM and CSF. For the comparison between SE-EPI and GE-EPI data, a paired *t*-test was conducted to detect statistically significant difference at various frequency offsets. The *P*-value threshold used in all the *t*-tests (including the one-sample *t*-test and the paired *t*-test) was set at 0.05, two-sided and corrected for multiple comparisons by Bonferroni correction.

RESULTS

Figure 1 shows the representative SE-EPI and GE-EPI images with and without the MT prepulse, and the corresponding MTR images of the ones with MT prepulse. Figure 2 shows the z-spectra (Fig. 2a and c) and the MTR_{asym} spectra (Fig. 2b and d) in the GM/WM and CSF, averaged over 14 subjects from the SE-EPI data. Figure 3 shows the results from the GE-EPI data. The z-spectra in CSF (Figs. 2c and 3c) are narrower than in GM/WM (Figs. 2a and 3a). In addition, the MR signal fraction M_{sat}/M_0 is near unity at off-resonance frequency offsets larger than 5 ppm (Figs. 2c and 3c), while the GM/WM has lower M_{sat}/M_0 (Figs. 2a and 3a). Furthermore, the statistical analysis from SE-EPI showed that the z-spectrum in the GM/WM (Fig. 2b) was asymmetrical about the water resonance frequency ($P < 0.05$). A larger saturation effect was observed on the negative offset side at the frequency offsets of 15–30 ppm, 65 ppm, and 75 ppm (minimum: –1.9% at 22.6 ppm) and on the positive offset side at 2 ppm, 3 ppm, and 3.5–5.5 ppm (maximum: 6.8% at 3.9 ppm). There was no significant difference of MTRs between corresponding negative and positive frequency offsets in CSF (Fig. 2d).

The GE-EPI data showed similar results as the SE-EPI data. The statistical analysis from GE-EPI showed that the z-spectrum in the GM/WM (Fig. 3b) was asymmetrical ($P < 0.05$). A larger saturation effect was similarly observed on the negative offset side at 10–30 ppm, 40 ppm, 50 ppm, 65 ppm, and 70 ppm (minimum: –1.4% at 24.5 ppm), and on the positive offset side between 1.5 and 4ppm (maximum: 3.3% at 3.6 ppm). The z-spectrum of CSF did not show any asymmetry around water resonance, except at frequency offsets of

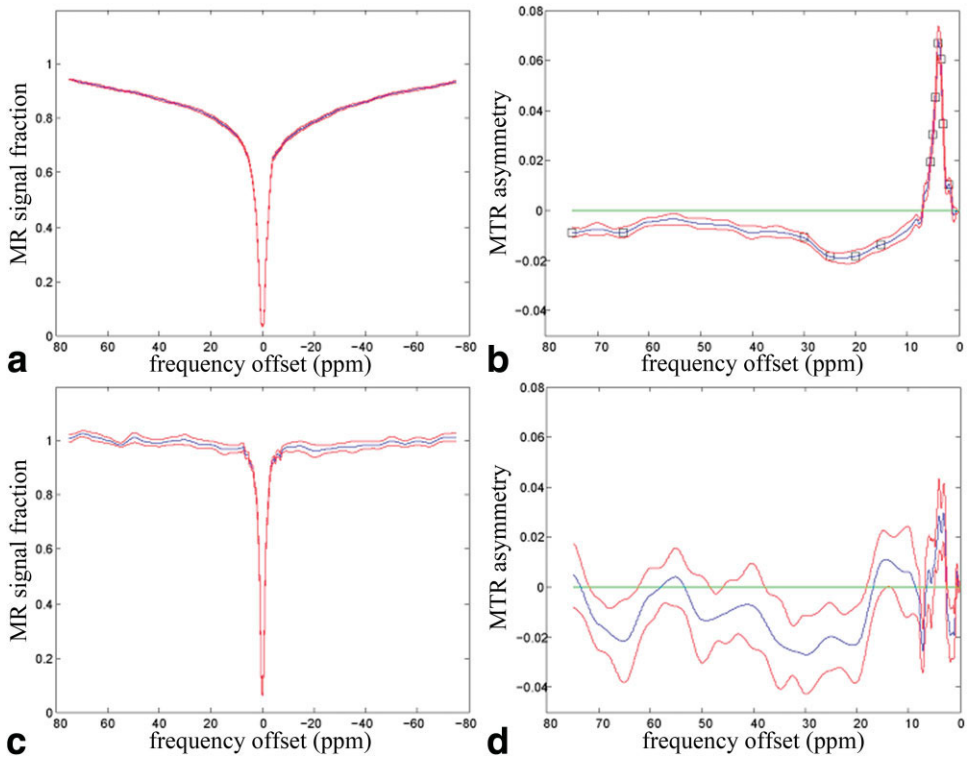

Figure 2. MT asymmetry results from SE-EPI data ($N = 14$): (**a**) mean z-spectrum (blue line) with standard error of the mean (SEM; red line) of GM/WM from C3/C4–C5; (**b**) mean MTR asymmetry with SEM in GM/WM (the black square on the curve highlights the point that the MTR asymmetry values at those particular frequency offsets are significantly different from zero by one-sample *t*-test [$P < 0.05$]); (**c**) mean z-spectrum with SEM in CSF; and (**d**) mean MTR asymmetry with SEM in CSF. [Color figure can be viewed in the online issue, which is available at www.interscience.wiley.com.]

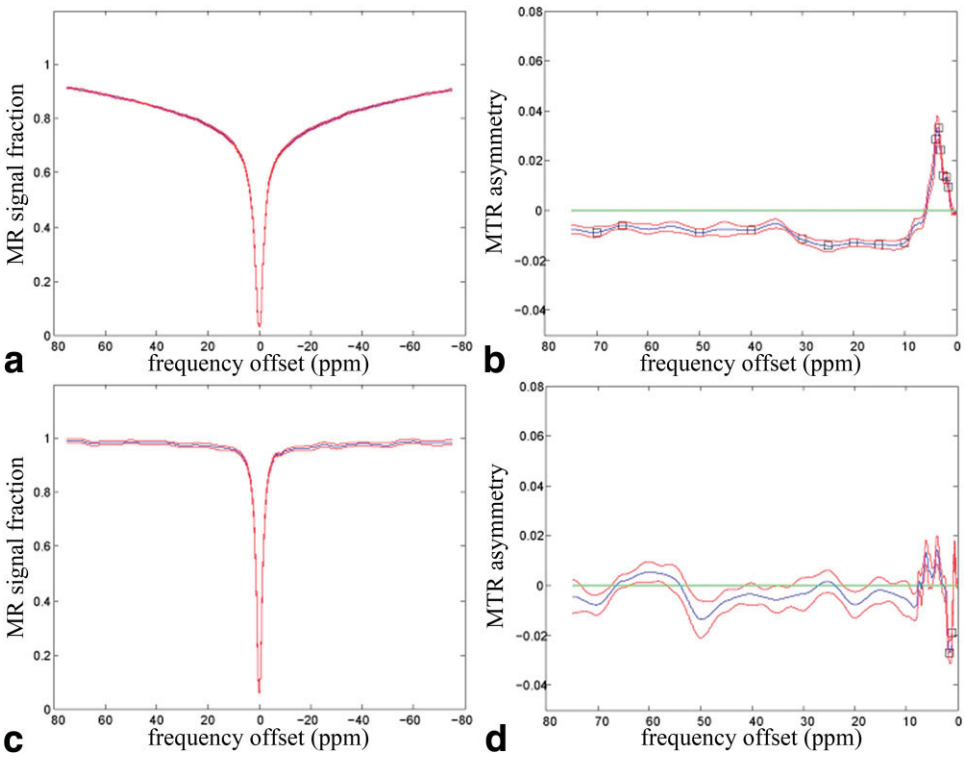

Figure 3. MT asymmetry results from GE-EPI data (N = 14): (a) mean z-spectrum (blue line) with the SEM (red line) of GM/WM from C3/C4–C5; (b) mean MTR asymmetry with SEM in GM/WM (the black square on the curve highlights the point that the MTR asymmetry values at those particular frequency offsets are significantly different from zero by one-sample t-test [$P < 0.05$]); (c) mean z-spectrum with SEM in CSF; and (d) mean MTR asymmetry with SEM in CSF.

1 and 1.5 ppm (Fig. 3d). Figure 4 shows the difference of MTR_{asym} values obtained in SE-EPI and GE-EPI sequences in GM/WM and CSF respectively. The MTR_{asym} values in GM/WM obtained in SE-EPI were significantly higher than the ones in GE-EPI at frequency offsets between 3.5 and 4.5 ppm ($P < 0.05$).

DISCUSSION

The current MT asymmetry study was carried out in the human cervical spinal cord at 3T using SE-EPI and GE-EPI with an MT prepulse. Our results demonstrated MTR asymmetry in the GM/WM due to both conventional MT and CEST effects. The comparison of MTR_{asym} between SE-EPI and GE-EPI further suggested that while both sequences had similar trends in the results, SE-EPI showed significantly higher MTR asymmetry than GE-EPI at the frequency range of the amide protons.

The GM/WM mainly consists of axons, dendrites, and cell bodies of the neural cells, which are composed of various proteins, peptides, and macromolecules. Therefore, the MT effect exists through chemical exchange and cross-relaxation. On the other hand, CSF

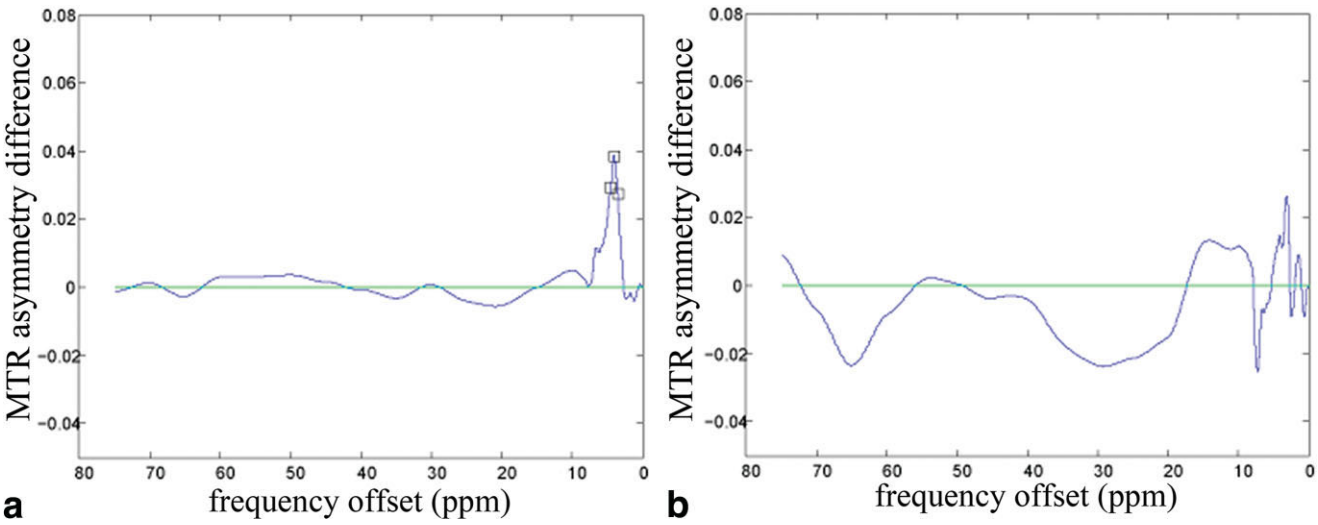

Figure 4. Comparison of MTR asymmetry (MTR_{asym}) between SE-EPI and GE-EPI by paired t-test (SE – GE): (a) in GM/WM of the cervical spinal cord; (b) in CSF. The black square on the curve shows that the MTR_{asym} values obtained from SE and GE are significantly different at that particular frequency offset by paired t-test ($P < 0.05$).

consists mainly of water. The concentration of proteins and amino acid in CSF is very low, so there is insignificant MT. This explains the negligible MT effect in the CSF, which leads to a narrower z-spectrum when compared with the GM/WM and the MR signal fraction M_{sat}/M_0 is driven to unity at off-resonance frequency offsets larger than 5 ppm (Figs. 2c and 3c). When comparing the MTR_{asym} values between GM/WM and CSF in SE-EPI (Fig. 2b and d) and GE-EPI (Fig. 3b and d), the z-spectrum in the GM/WM was asymmetrical about the water resonance frequency, with more saturation effect at the lower frequencies (corresponding to a negative frequency offset) far away from water and at higher frequencies (a positive frequency offset) close to water. These results are consistent with previous studies on the brain (7,8). The larger saturation effect at the negative offset frequencies far away from water was attributed to a center frequency shift from the semisolid pool with respect to water in conventional MT (7). The larger saturation effect at the positive offset frequencies close to water is more complicated. Both the conventional MT asymmetry and the CEST effect, e.g., the amide proton transfer (APT) effect at +3.5 ppm (10), contribute to this effect. Our results demonstrated the MT asymmetry in the GM/WM of human cervical spinal cord arising from both conventional MT and CEST effects. The CSF did not have a significant MT asymmetry at frequency offsets around 3.5 ppm and >10 ppm, as CSF had very little conventional MT and CEST effects. However, it is noted that the MTR_{asym} value was significantly different from zero in CSF at frequencies very close to the water resonance (1 ppm and 1.5 ppm in Fig. 3d) in GE-EPI. This may be due to the large standard deviation (SD) in MTR_{asym} in CSF (18). In the literature, artifacts in CSF in APT-weighted images have been well documented (10,14,18).

In the comparison between GE and SE data, the paired *t*-test showed that SE has significantly higher MTR_{asym} than GE in GM/WM between 3.5 ppm and 4.5 ppm (Fig. 4). This frequency range corresponds mainly to the amide protons. This suggests that the detecting sensitivity of the APT effect in the cervical spinal cord may be higher in the SE-EPI sequences. This can be explained by the fact that the cervical spinal cord is subjected to considerable magnetic field inhomogeneity because of the large susceptibility difference among the tissues. This problem can be minimized by using an SE-based sequence. Due to the presence of the 180° refocusing pulse, SE sequence can produce images with less intensity distortion, thus increasing the detecting sensitivity of MT asymmetry.

There are several limitations in our experiments. First, the cross-sectional diameter of the spinal cord is very small (~10 mm), and single-shot EPI was used for fast imaging in the current study. Because of the long echo train length compared with the conventional imaging, EPI suffers from spatial blurring and susceptibility-induced distortion, especially in the cervical spinal cord (19,20). Also, due to the high sensitivity of MTR to motion (21), it is not easy to separate the GM and WM to perform respective MT asymmetry analyses. Therefore, in this study, the GM and WM were combined together. Second, physiological motion arising from blood, CSF flow, and breathing can decrease the sensitivity of asymmetry detection. Therefore, VCG triggering during data acquisition and image registration were used to reduce the physiological motion. Respiratory triggering was not used in this study, as a recent study in spinal functional MRI (fMRI) suggested that motion from respiration is not a significant source of artifact (22).

The prephasing gradient lobe for phase-encoding in the default SE-EPI setting of our MR system is placed before the 180° refocusing pulse. However, in the current study, it was moved to a position after the refocusing pulse. The advantage of this was to reduce the oblique flow displacement artifact (16) induced mainly from CSF. However, there was a disadvantage in doing so. The free-induction decay (FID) from the nonideal refocusing pulse (flip angle ≠ 180°) would also be phase-encoded, which might result in image artifacts (16). However, from our images, no significant artifact was observed in the spinal cord.

The T1s of WM and GM in the cervical cord at 3T are around 860 msec and 980 msec, respectively (23). Therefore, using a TR of 2 heartbeats in the current study would mean that the images would have some T1 weighting. Due to the variation of heart rates of different subjects, the T1 contrast would vary among subjects. However, this would have a minimal effect on the MT asymmetry analysis as the MTR was calculated by taking the ratio of two images, which can remove the inferred T1 weighting (21).

The significance of this study is that the existence of MT asymmetry in the human cervical spinal has been verified. The conventional MT asymmetry may give more insight into the interaction between semisolid tissue components and bulk water, providing a new MR contrast in certain pathology that affects the macromolecule pool or the chemical shift difference between the bulk water pool and the solid-like macromolecule pool (8). The CEST effect, more specifically APT, provides a method for detecting endogenous mobile proteins and peptides at a very low concentration through the water signal. It can be used to image tissue pH (10), tissue protein, and peptide content (15). Moreover, the discovery of the MT asymmetry around the water resonance also necessitates more sophistication in some MRI experiments. For example, MT asymmetry adversely affects the accuracy of perfusion quantification in continuous-wave arterial spin labeling (CASL). Compensation schemes (24,25) such as gradient inversion (6), compensated $\delta\omega_2$ inversion (6), and a two-coil approach (25) have to be used. The conventional MT asymmetry will also complicate the quantification of CEST effect, as the two are concurrent. The proper algorithm has to be derived in order to separate the conventional MT asymmetry and CEST in the future.

In conclusion, MT asymmetry has been demonstrated in GM/WM of human cervical spinal cord at 3T. Both SE-EPI and GE-EPI showed consistent results. There was a larger saturation effect at the negative frequency offsets far away from water, which was attributed to a center frequency shift from the semisolid macromolecule pool with respect to water in conventional MT. A larger saturation effect was also observed

at the positive offset frequencies close to water, which was attributed mainly to a type of CEST effect, the APT effect. Results obtained using an SE sequence showed significantly higher MTR_{aysm} than GE at the amide proton frequency range, possibly due to less intensity distortion in SE.

ACKNOWLEDGMENTS

We acknowledge the 3T MRI Unit, University of Hong Kong, for support in the use of the scanner. We also thank Mr. Tsz-Kit Cheung, Mr. Ting-Hung Li, and Mr. Li Hu for their help in the preparation of the experiment.

REFERENCES

1. Wolff SD, Balaban RS. Magnetization transfer contrast (MTC) and tissue water proton relaxation in vivo. Magn Reson Med 1989:10: 135–144.
2. Balaban RS, Ceckler TL. Magnetization transfer contrast in magnetic resonance imaging. Magn Reson Q 1992:8:116–137.
3. Bryant RG. The dynamics of water-protein interactions. Annu Rev Biophys Biomol Struct 1996:25:29–53.
4. Henkelman RM, Stanisz GJ, Graham SJ. Magnetization transfer in MRI: a review. NMR Biomed 2001:14:57–64.
5. Henkelman RM, Huang X, Xiang QS, Stanisz GJ, Swanson SD, Bronskill MJ. Quantitative interpretation of magnetization transfer. Magn Reson Med 1993:29:759–766.
6. Pekar J, Jezzard P, Roberts DA, Leigh JS, Jr., Frank JA, McLaughlin AC. Perfusion imaging with compensation for asymmetric magnetization transfer effects. Magn Reson Med 1996:35:70–79.
7. Hua J, Jones CK, Blakeley J, Smith SA, van Zijl PC, Zhou J. Quantitative description of the asymmetry in magnetization transfer effects around the water resonance in the human brain. Magn Reson Med 2007:58:786–793.
8. Hua J, van Zijl PC, Sun PZ, Zhou J. Quantitative description of magnetization transfer (MT) asymmetry in experimental brain tumors. In: Proceedings of the 15th Annual Meeting of ISMRM, Berlin, Germany, 2007 (Abstract 882).
9. Stein AD, Roberts DA, McGowan J, Reddy R, Leigh JS. Asymmetric cancellation of magnetization transfer effects. In: Proceedings of the 2nd Annual Meeting of Society of Magnetic Resonance, San Francisco, CA, USA, 1994 (Abstract 880).
10. Zhou J, Payen JF, Wilson DA, Traystman RJ, van Zijl PC. Using the amide proton signals of intracellular proteins and peptides to detect pH effects in MRI. Nat Med 2003:9:1085–1090.
11. Wolff SD, Balaban RS. NMR imaging of labile proton exchange. J Magn Reson 1990:86:164–169.
12. Guivel-Scharen V, Sinnwell T, Wolff SD, Balaban RS. Detection of proton chemical exchange between metabolites and water in biological tissues. J Magn Reson 1998:133:36–45.
13. Ward KM, Aletras AH, Balaban RS. A new class of contrast agents for MRI based on proton chemical exchange dependent saturation transfer (CEST). J Magn Reson 2000:143:79–87.
14. Zhou J, van Zijl PC. Chemical exchange saturation transfer imaging and spectroscopy. Prog Nucl Magn Reson Spectrosc 2006:48: 109–136.
15. Zhou J, Lal B, Wilson DA, Laterra J, van Zijl PC. Amide proton transfer (APT) contrast for imaging of brain tumors. Magn Reson Med 2003:50:1120–1126.
16. Bernstein MA, King KF, Zhou XJ. Handbook of MRI pulse sequences. Boston: Elsevier Academic Press; 2004. 1017 p.
17. Woods RP, Grafton ST, Watson JD, Sicotte NL, Mazziotta JC. Automated image registration: II. intersubject validation of linear and nonlinear models. J Comput Assist Tomogr 1998:22:153–165.
18. Zhou J, Wilson DA, Sun PZ, Klaus JA, Van Zijl PC. Quantitative description of proton exchange processes between water and endogenous and exogenous agents for WEX, CEST, and APT experiments. Magn Reson Med 2004:51:945–952.
19. Ng MC, Smith SA, Gillen JS, et al. Improved distortion correction in cerebral and spinal DTI using interleaved reversed gradients. In: Joint Annual Meeting ISMRM-ESMRB, Berlin, Germany, 2007 (Abstract 2124).
20. Voss HU, Watts R, Ulug AM, Ballon D. Fiber tracking in the cervical spine and inferior brain regions with reversed gradient diffusion tensor imaging. Magn Reson Imaging 2006:24:231–239.
21. Smith SA, Golay X, Fatemi A, et al. Magnetization transfer weighted imaging in the upper cervical spinal cord using cerebrospinal fluid as intersubject normalization reference (MTCSF imaging). Magn Reson Med 2005:54:201–206.
22. Stroman PW. Discrimination of errors from neuronal activity in functional MRI of the human spinal cord by means of general linear model analysis. Magn Reson Med 2006:56:452–456.
23. Smith SA, Edden RA, Farrell JA, Barker PB, Van Zijl PC. Measurement of T1 and T2 in the cervical spinal cord at 3 Tesla. Magn Reson Med 2008:60:213–219.
24. Pekar J, Jezzard P, Roberts DA, et al. Perfusion imaging with MTC offset compensation. In: Proceedings of the 2nd Annual Meeting of SMR, San Francisco, CA, USA, 1994 (Abstract 281).
25. Detre JA, Zhang W, Roberts DA, et al. Tissue specific perfusion imaging using arterial spin labeling. NMR Biomed 1994:7:75–82.